Inorg. Chem. **2008**, *47*, 1653−1662

Infrared Spectra of Methylidynes Formed in Reactions of Re Atoms with Methane, Methyl Halides, Methylene Halides, and Ethane: Methylidyne C−H Stretching Absorptions, Bond Lengths, and s Character

Han-Gook Cho[†] **and Lester Andrews***[,‡]

Department of Chemistry, University of Incheon, 177 Dohwa-dong, Nam-ku, Incheon, 402-749, South Korea, and Department of Chemistry, University of Virginia, P.O. Box 400319, Charlottesville, Virginia 22904-4319

Received July 27, 2007

Rhenium carbyne complexes ($HC{\equiv}ReH_3$, $HC{\equiv}ReH_2X$, $HC{\equiv}ReHX_2$, [X = F, Cl, and Br] and $CH_3C{\equiv}ReH_3$) are produced by reactions of laser-ablated Re atoms with methane, methyl halides, methylene halides, and ethane via oxidative C−H(X) insertion and α-hydrogen migration in favor of the carbon−metal triple bond. The stabilities of the carbyne complexes relative to other possible products are predicted by DFT calculations. The diagnostic methylidyne C−H stretching absorptions of $HC{\equiv}ReH_3$ and its mono- and dihalo derivatives are observed on the blue sides of the precursor C−H stretching bands, and the frequency decreases and the bond length increases in the order of H, F, Cl, and Br, following the decreasing s character in hybridization for the C−H bond. The dihalo methylidynes have higher C−H stretching frequencies and s characters than the monohalo species. The rhenium methylidynes have C_s structures, and as a result the $HC{\equiv}ReH_3$ and $CH_3C{\equiv}ReH_3$ complexes have two equivalent shorter and one longer Re−H bonds, as compared to the tungsten methylidyne $HC{\equiv}WH_3$ with three equivalent W−H bonds.

Introduction

The discovery of transition metal complexes with carbon−metal multiple bonds in the 1970s has opened exciting new fields in chemistry, including alkene metathesis and alkane C−H insertion.[1] The numerous carbyne complexes have been introduced to show their versatile chemistry and catalytic activities,[2] but only a few of them contain the simple M≡C−H or M≡C−CH_3 moiety (M = transition metal).[3] Moreover, the methylidyne C−H vibrational characteristics remain largely uninvestigated owing in part to very low infrared intensity and to interference from other hydrogen stretching absorptions, whereas the stronger C≡M stretching bands are observed and frequently used as a probe, but these often suffer from ligand effects.[4,5]

The *trans*-W(≡CH)$(PMe_3)_4Cl$ complex with deuteriated methyl groups has been prepared, and the weak methylidyne C−H stretching band near 2980 cm^{-1} and its deuterium counterpart at 2240 cm^{-1} were assigned by the Hopkins group.[6] Bond lengths in the H−C≡W moiety for a related complex were later measured by neutron diffraction.[7] Recently, small carbene and carbyne complexes ($CH_2{=}MH_2$, $HC{\equiv}MH_3$, and their halide derivatives) have been prepared

* To whom correspondence should be addressed. E-mail: lsa@virginia.edu.
† University of Incheon.
‡ University of Virginia.

(1) (a) Schrock, R. R. *Chem. Rev.* **2002**, *102*, 145. (b) Herndon, J. W. *Coord. Chem. Rev.* **2007**, *251*, 1158. (c) Herndon, J. W. *Coord. Chem. Rev.* **2006**, *250*, 1889. (d) Herndon, J. W. *Coord. Chem. Rev.* **2005**, *249*, 999. (e) Herndon, J. W. *Coord. Chem. Rev.* **2004**, *248*, 3. (f) Da Re, R. E.; Hopkins, M. D. *Coord. Chem. Rev.* **2005**, *249*, 1396.
(2) (a) Fischer, E. O.; Kreis, G.; Kreiter, C. G.; Müller, J.; Huttner, G.; Lorenz, H. *Angew. Chem., Int. Ed. Engl.* **1973**, *12*, 564 (carbyne synthesis). (b) McLain, S. J.; Wood, C. D.; Messerle, L. W.; Schrock, R. R.; Hollander, F. J.; Youngs, W. J.; Churchill, M. R. *J. Am. Chem. Soc.* **1978**, *100*, 5962 (carbyne synthesis).
(3) Nugent, W. A.; Mayer, J. M. *Metal-Ligand Multiple Bonds*; John Wiley and Sons: New York, 1988.
(4) Barnes, D.; Gillett, D. A.; Merer, A. J.; Metha, G. F. *J. Chem. Phys.* **1996**, *105*, 6168 (W≡CH).
(5) (a) Mavridis, A.; Alvarado-Swaisgood, A. E.; Harrison, J. F. *J. Phys. Chem.* **1986**, *90*, 2584 (M≡CH^+). (b) Kalemos, A.; Dunning, Jr., T. H.; Harrison, J. F.; Mavridis, A. *J. Chem. Phys.* **2003**, *119*, 3745 (Ti≡CH). (c) Barnes, M.; Merer, A. J.; Metha, G. F. *J. Mol. Spectrosc.* **1997**, *181*, 168 (Ti≡CH). (d) Sari, L.; Yamaguchi, Y.; Schaefer, H. III *J. Chem. Phys.* **2001**, *115*, 5932 (HC≡Ge). (e) Fujitake, M.; Echizenya, R.; Shirai, T.; Kurita, S.; Ohashi, N. *J. Mol. Spectrosc.* **2004**, *223*, 113 (HC≡Si).
(6) Manna, J.; Dallinger, R. F.; Miskowski, V. M.; Hopkins, M. D. *J. Phys. Chem. B* **2000**, *104*, 10928 ((H−C≡W)$(PMe_3)_4Cl$).

10.1021/ic701505w CCC: $40.75
Published on Web 02/08/2008

in reactions of Group 3–6 metal atoms with methane and methyl halides, showing interesting structures and fascinating photochemistry.[8] Particularly, Group 5 and 6 metals have formed anionic and neutral methylidyne complexes ($HC{\equiv}MH_3^-$, $HC{\equiv}MH_3$, and their halide derivatives), respectively. More recently, rhenium atom reactions with CHX_3 and CX_4 precursors (X = F and Cl) have produced the halogen substituted $HC{\equiv}ReX_3$ and $XC{\equiv}ReX_3$ complexes, and calculations show that spin–orbit coupling is not strong enough to override significant Jahn–Teller distortion.[9]

Here, we report the formation and IR spectra of $HC{\equiv}ReH_3$, $HC{\equiv}ReH_2F$, $HC{\equiv}ReH_2Cl$, $HC{\equiv}ReH_2Br$, $HC{\equiv}ReHF_2$, $HC{\equiv}ReHFCl$, $HC{\equiv}ReHCl_2$ and $CH_3C{\equiv}ReH_3$ in reactions of laser-ablated Re atoms with methane, methyl and methylene halides, and ethane. The elusive methylidyne C−H stretching absorptions are observed from $HC{\equiv}ReH_3$ and its halide derivatives, and these frequencies show a decreasing trend with the order of H, F, Cl, and Br. Only the s character in the C−H bond among the molecular properties varies consistently with the frequency. In addition, the di- and trihydrido complexes provide model systems for comparison with larger ligated monohydrido and dihydrido alkylidyne compexes.[10] A preliminary account of the Re and methane reaction system has been communicated.[11]

Experimental and Computational Methods

Laser ablated Re atoms (Johnson−Matthey) were reacted with CH_4 (Matheson, UHP grade), (CH_3X (Matheson), CD_3F (synthesized from CD_3Br and HgF_2)), $^{13}CH_3F$, CD_3Br, CD_2Cl_2, $^{13}CH_2Cl_2$ (Cambridge Isotopic Laboratories, 99%), CD_3Cl (synthesized from CD_3Br and $HgCl_2$), CH_2F_2, CH_2FCl (Du Pont), CD_2FCl (synthesized from CD_2Cl_2 and HgF_2), and CH_2Cl_2 (Fisher) in excess argon during condensation at 8 K. These methods have been described in detail elsewhere.[12] Reagent gas mixtures were typically 0.5% in argon. After reaction, infrared spectra were recorded at a resolution of 0.5 cm^{-1} using a Nicolet 550 spectrometer with an MCT-B detector. Samples were later irradiated for 20 min periods by a mercury arc lamp (175 W) with the globe removed and a combination of optical filters and subsequently annealed to allow further reagent diffusion.

Complementary density functional theory (DFT) calculations were carried out using the Gaussian 03 package,[13] B3LYP density functional, 6–311++G(3df,3pd) basis sets for C, H, F, Cl, and Br[13] and the SDD pseudopotential and basis set[14] for Re to provide a consistent set of vibrational frequencies for the reaction products. Geometries were fully relaxed during optimization, and the optimized geometry was confirmed by vibrational analysis. Anharmonic frequency calculations by numerical differentiation[15] (with Gaussian 03 keyword "anharmonic") were also carried out with B3LYP to compare with experimental values and to examine the effects of anharmonicity. BPW91,[16] MP2,[17] and CCSD[18] calculations were also done to confirm the B3LYP results. All of the vibrational frequencies were calculated analytically. In the calculation of binding energy of a metal complex, the zero-point energy is included.

Results and Discussion

The major product in the reaction of laser-ablated Re atoms and methane, methyl halides, methylene halides or ethane will be identified from the effect of isotopic substitution on the matrix infrared spectra and comparison with frequencies calculated by density functional theory. Weak absorptions were detected at 932.3 and 931.7 cm^{-1} for the very strong antisymmetric stretching mode of $^{185}ReO_2$ and $^{187}ReO_2$ from the reaction with trace oxygen impurity in the argon matrix gas.[19a]

Re + CH_4. Infrared spectra for the $HC{\equiv}ReH_3$ product of laser-ablated Re atom reaction with CH_4, $^{13}CH_4$, CD_4, and CH_2D_2 have been reported in our communication.[11] The methylidyne C−H stretching absorption was observed at 3101.8 cm^{-1} with deuterium and ^{13}C counterparts at 2334.3 and 3090.8 cm^{-1} (H/D and $^{12}C/^{13}C$ ratios of 1.329 and 1.004), respectively. This C−H stretching frequency is substantially (about 200 cm^{-1}) higher than those of normal saturated hydrocarbons, because of higher s character in the C−H bond arising from interaction with the adjacent multiple carbon-rhenium bond.[3,20] The C−H stretching mode is predicted by DFT in the harmonic approximation at 3264.3 cm^{-1}, which is 5.2% higher and in accord with expectations.[21] Notice, however, that anharmonic frequency calculations

(7) Ménoret, C.; Spasojević-de Bire, A.; Dao, N. Q.; Cousson, A.; Kiat, J.-M.; Manna, J. D.; Hopkins, M. D. *J. Chem. Soc., Dalton Trans.* **2002**, 3731 ($BrW{\equiv}CH(dmpe\text{-}d_{12})_2$).

(8) Andrews, L.; Cho, H.-G. *Organometallics* **2006**, *25*, 4040 and references therein.

(9) Lyon, J. T.; Cho, H.-G.; Andrews, L.; Hu, H.-S.; Li, J *Inorg. Chem.* **2007**, *46*, 8728 (Re + CHX_3).

(10) (a) Ozerov, O. V.; Watson, L. A.; Pink, M.; Caulton, K. G *J. Am. Chem. Soc.* **2004**, *126*, 6363. (b) Leeaphon, M.; Fanwick, P. E.; Walton, R. A. *J. Am. Chem. Soc.* **1992**, *114*, 1890.

(11) Cho, H.-G.; Andrews, L. *Organometallics* **2007**, *26*, 4098 ($HC{\equiv}ReH_3$).

(12) (a) Andrews, L.; Citra, A *Chem. Rev.* **2002**, *102*, 885 and references therein. (b) Andrews, L *Chem. Soc. Rev* **2004**, *33*, 123 and references therein. (c) Andrews, L.; Willner, H.; Prochaska, F. T. *J. Fluorine Chem.* **1979**, *13*, 273.

(13) Kudin, K. N.; Burant, J. C.; Millam, J. M.; Iyengar, S. S.; Tomasi, J.; Barone, V.; Mennucci, B.; Cossi, M.; Scalmani, G.; Rega, N.; Petersson, G. A.; Nakatsuji, H.; Hada, M.; Ehara, M.; Toyota, K.; Fukuda, R.; Hasegawa, J.; Ishida, M.; Nakajima, T.; Honda, Y.; Kitao, O.; Nakai, H.; Klene, M.; Li, X.; Knox, J. E.; Hratchian, H. P.; Cross, J. B.; Adamo, C.; Jaramillo, J.; Gomperts, R.; Stratmann, R. E.; Yazyev, O.; Austin, A. J.; Cammi, R.; Pomelli, C.; Ochterski, J. W.; Ayala, P. Y.; Morokuma, K.; Voth, G. A.; Salvador, P.; Dannenberg, J. J.; Zakrzewski, V. G.; Dapprich, S.; Daniels, A. D.; Strain, M. C.; Farkas, O.; Malick, D. K.; Rabuck,A. D.; Raghavachari, K.; Foresman, J. B.; Ortiz, J. V.; Cui, Q.; Baboul, A. G.; Clifford, S.; Cioslowski, J.; Stefanov, B. B.; Liu, G.; Liashenko, A.; Piskorz, P.; Komaromi, I.; Martin, R. L.; Fox, D. J.; Keith, T.; Al-Laham, M. A.; Peng, C. Y.; Nanayakkara, A.; Challacombe, M.; Gill, P. M. W.; Johnson, B.; Chen, W.; Wong, M. W.; Gonzalez, C.; Pople, J. A. Gaussian 03 Revision B.04, Gaussian, Inc.: Pittsburgh, Pennsylvania, 2003.

(14) (a) Becke, A. D. *J. Chem. Phys.* **1993**, *98*, 5648. (b) Lee, C.; Yang, Y.; Parr, R. G. *Phys. Rev. B* **1988**, *37*, 785. (c) Frisch, M. J.; Pople, J. A.; Binkley, J. S. J. *Chem. Phys.* **1984**, *80*, 3265. (d) Raghavachari, K.; Trucks, G. W. *J. Chem. Phys.* **1989**, *91*, 1062. (e) Andrae, D.; Haeussermann, U.; Dolg, M.; Stoll, H.; Preuss, H. *Theor. Chim. Acta* **1990**, *77*, 123.

(15) Page, M.; Doubleday, C.; McIver, J. W. Jr. *J. Chem. Phys.* **1990**, *93*, 5634.

(16) Burke, K.; Perdew, J. P.; Wang, Y. In *Electronic Density Functional Theory: Recent Progress and New Directions*; Dobson, J. F., Vignale, G., Das, M. P. Eds.; Plenum, **1998**.

(17) Frisch, M. J.; Head-Gordon, M.; Pople, J. A. *Chem. Phys. Lett.* **1990**, *166*, 281.

(18) Pople, J. A.; Krishnan, R.; Schlegel, H. B.; Binkley, J. S. *Int. J. Quantum Chem.* **1978**, *14*, 545.

(19) (a) Zhou, M.; Citra, A.; Liang, B.; Andrews, L. *J. Phys. Chem A.* **2000**, *104*, 3457 (Re + O_2). (b) Wang, X.; Andrews, L *J. Phys. Chem. A* **2003**, *107*, 4081 (Re + H_2).

(20) Pavia, D. L.; Lampman, G. M.; George, S. K. *Introduction to Spectroscopy*, 3rd ed.; Brooks Cole: New York, 2000.

(21) (a) Scott, A. P.; Radom, L. *J. Phys. Chem.* **1996**, *100*, 16502. (b) Andersson, M. P.; Uvdal, P. L. *J. Phys. Chem. A* **2005**, *109*, 3937.

Table 1. Observed and Calculated Fundamental Frequencies (cm^{-1}) of $HC{\equiv}ReH_3$ Isotopomers in the Ground $^2A'$ Electronic State[a]

	$HC{\equiv}ReH_3$				$DC{\equiv}ReD_3$			$H^{13}C{\equiv}ReH_3$			CH_2D_2
approximate description	obs	anharm	harm	int	obs	harm	int	obs	harm	int	obs
A′ C−H str.	3101.8	3118.0	3264.3	36	2334.3	2430.5	25	3090.8	3252.1	35	3101.9, 2334.3
A′ ReH_2 str.	1946.4	2010.7	2088.8	76	1399.3	1481.4	40	1946.4	2088.8	76	
A′ ReH str.	1809.9, 1804.0	1781.8	1855.7	244	1302.6, 1298.1	1318.1	121	1809.9, 1803.9	1855.7	244	1808.5, 1882.1, 1300.2
A′ C≡Re str.	1048.8	1092.9	1096.8	10	[b]	1041.2	7	1012.9	1061.4	9	[b]
A′ ReH_3 deform		732.3	751.4	2		549.6	0		749.5	2	
A′ HCRe bend		559.6	603.7	56		447.9	24		601.7	56	
A′ ReH_3 rock		454.1	492.3	24		368.6	18		489.3	23	
A′ ReH_2 scis.		447.6	459.5	2		325.9	1		459.5	2	
A″ ReH_2 str.	1910.1	1967.3	2040.3	46	1370.8	1449.0	24	1910.1	2040.2	46	
A″ ReH_2 twist		883.6	830.3	0		637.8	4		825.1	0	
A″ HCRe bend		661.4	695.7	109		501.6	56		694.1	108	
A″ ReH_3 rock		272.2	304.6	23		218.3	11		304.5	23	

[a] Observed in an argon matrix. Frequencies and intensities (km/mol) computed with in harmonic approximation using B3LYP/6–311++G(3df, 3pd)/SDD except where noted anharmonic. $HC{\equiv}ReH_3$ has a $C_s$structure with two equal Re-H bonds, and symmetry notations are based on the C_s structure. [b] Covered by precursor band.

(Table 1) locate the C−H stretching frequency at 3118.0 cm^{-1}, which is only 0.5% higher and demonstrates that the C−H vibration contains considerable anharmonicity.

The strongest absorption is split by the matrix cage at 1809.9 and 1804.0 cm^{-1}, which shifts upon deuterium substitution to 1302.5 and 1298.1 cm^{-1} (H/D ratios of 1.390 for a heavy metal hydride), and the ^{13}C counterparts show no isotopic shifts. These bands are due to a unique Re−H stretching absorption, and they indicate that oxidative C−H insertion by a Re atom clearly occurs. Two weaker product absorptions at 1946.4 and 1910.1 cm^{-1} are also appropriate for Re−H stretching modes. These weaker Re−H stretching absorptions are consistent with the predicted symmetric and antisymmetric Re−H stretching frequencies for the ReH_2 subunit with equivalent Re−H bonds in $HC{\equiv}ReH_3$, as shown in Table 1 (predicted 6.8 and 6.3% higher). Anharmonic frequency calculations find values that are only about 3% higher than observed, which verifies the anharmonic nature of these metal hydride modes.

An important weak absorption at 1048.8 cm^{-1} has its ^{13}C counterpart at 1012.9 cm^{-1}. These bands are due to the C≡Re stretching mode. The observed ^{13}C isotopic shift (35.9 cm^{-1}) is almost that computed for a pure C−Re stretching mode [38.6 cm^{-1}]. This diagnostic mode can appear only for a methylidyne product.[11] The calculated band position (1096.8 cm^{-1}) is slightly higher, as expected for density functional theory,[21] and the calculated ^{13}C shift for the methylidyne (35.4 cm^{-1}) is in excellent agreement with the observed shift for the $HC{\equiv}ReH_3$ molecule.

Re + CH_3X. Figure 1 illustrates isotopic methyl halide spectra in the C−H stretching regions. The product absorption marked "**y**" increases about 30% upon UV photolysis regardless of the reactant. CH_3F and CH_3Cl give similar yields whereas CH_3Br shows a relatively lower yield. The C−H stretching frequencies of 3092.9, 3090.1, and 3089.8 cm^{-1} in the CH_3F, CH_3Cl, and CH_3Br reaction product spectra are 8.9, 11.7, and 12.0 cm^{-1} lower, respectively, than the C−H mode at 3101.8 cm^{-1} in the $HC{\equiv}ReH_3$ spectrum. Similarly the C−D stretching frequencies of 2327.0, 2324.7, and 2324.4 cm^{-1} in the CD_3F, CD_3Cl, and CD_3Br spectra (H/D ratios of 1.329) are 7.3, 9.6, and 9.9 cm^{-1} lower than that of 2334.3 cm^{-1} in the CD_4 spectra, respectively. The

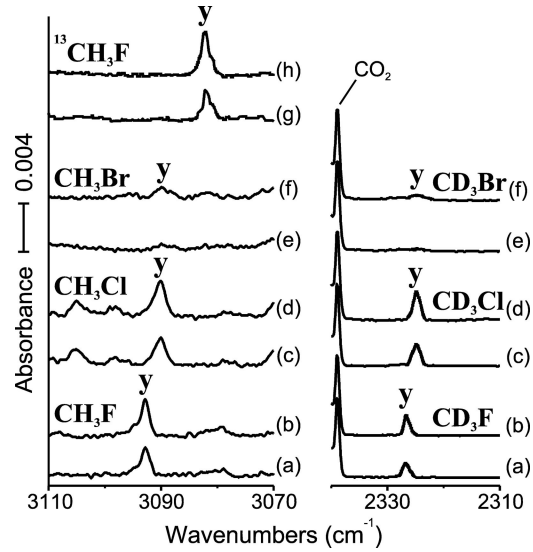

Figure 1. The C−H and C−D stretching regions for the laser-ablated Re atom reaction products with CH_3X or CD_3X (X = F, Cl, and Br) in excess argon at 8 K and their variation on UV ($240 < \lambda < 380$ nm) photolysis. (a) Re + 0.5% CH_3F or CD_3F in Ar codeposited for 1 h. (b) After photolysis. (c) Re + 0.5% CH_3Cl or CD_3Cl in Ar codeposited for 1 h. (d) After photolysis. (e) Re + 0.5% CH_3Br or CD_3Br in Ar codeposited for 1 h. (f) After photolysis. (g) Re + 0.5% $^{13}CH_3F$ in Ar codeposited for 1 h, and (h) After photolysis. The **y** label indicates the methylidyne product absorptions.

^{13}C substitution for CH_3F leads to a red shift of 10.8 cm^{-1} ($^{12}C/^{13}C$ ratio of 1.0035), which is close to the calculated 12.0 cm^{-1} shift.

On the basis of the frequencies being higher than for C−H stretching frequencies for saturated hydrocarbons and their variation upon halide and isotopic substitution, the above observed absorptions verify that a primary reaction product containing a single C−H bond with higher s character ($HC{\equiv}ReH_2X$) is also formed in reactions of methyl halides, parallel to the case of $HC{\equiv}ReH_3$. No other strong product absorptions are observed in the Re + CH_3X spectra, in contrast to the previous results of Group 3–6 metals, which also reveal Grignard-type insertion ($CH_3{-}ReX$) and methylidene ($CH_2{=}ReHX$) complexes in addition to the methylidyne ($HC{\equiv}ReH_2X$) products.[8]

The high preference for the C≡Re triple bond is predicted from the low carbyne energy in DFT calculations, in line

Table 2. Observed and Calculated Fundamental Frequencies (cm^{-1}) of $HC{\equiv}ReH_2F$ Isotopomers in the Ground $^2A'$ Electronic State[a]

approximate description	$HC{\equiv}ReH_2F$ obs	$HC{\equiv}ReH_2F$ anharm[b]	$HC{\equiv}ReH_2F$ harm	$HC{\equiv}ReH_2F$ int	$DC{\equiv}ReD_2F$ obs	$DC{\equiv}ReD_2F$ harm	$DC{\equiv}ReD_2F$ int	$H^{13}C{\equiv}ReH_2F$ obs	$H^{13}C{\equiv}ReH_2F$ harm	$H^{13}C{\equiv}ReH_2F$ int
A′ C−H str.	3092.9	3095.7	3249.7	24	2327.0	2418.5	18	3082.1	3237.7	23
A′ ReH_2 str.	[c]	2091.6	2155.3	52	1480.2	1529.8	27	2063.7	2155.3	52
A′ C≡Re str.		1066.9	1081.6	7		1030.7	6		1045.8	7
A′ HCRe bend		782.7	821.1	3	620.7	636.1	13		815.6	2
A′ ReH_2 wag	612.7	620.8	636.8	24		430.0	55	612.5	636.2	25
A′ ReF str.	573.2, 566.4	570.6	574.4	168	608.5, 606.6	608.7	94	572.6, 565.8	573.9	168
A′ ReH_2 scis.		373.9	472.4	5		335.7	1		472.4	5
A′ CReF bend		175.9	176.0	5		167.4	5		173.1	5
A″ ReH_2 str.	2041.0	2059.2	2126.4	38	1459.2	1508.6	20	2040.4	2126.3	38
A″ HCRe bend		827.4	853.0	8		671.0	6		845.4	8
A″ ReH_2 twist	632.3	613.6	639.2	50		454.0	25	631.8	639.1	50
A″ ReH_2 rock		178.4	255.5	7		194.8	4		255.1	7

[a] Observed in an argon matrix. Frequencies and intensities are for harmonic DFT calculations except where otherwise noted. $HC{\equiv}ReH_2F$ has a C_s structure with two equal Re−H bonds. The symmetry notations are based on the C_s structure. [b] Calculated anharmonic frequencies. [c] Covered by precursor band.

Table 3. Observed and Calculated Fundamental Frequencies (cm^{-1}) of $HC{\equiv}ReH_2Cl$ Isotopomers in the Ground $^2A'$ Electronic State[a]

approximate description	$HC{\equiv}ReH_2Cl$ obs	$HC{\equiv}ReH_2Cl$ anharm[b]	$HC{\equiv}ReH_2Cl$ harm	$HC{\equiv}ReH_2Cl$ int	$DC{\equiv}ReD_2Cl$ obs	$DC{\equiv}ReD_2Cl$ harm	$DC{\equiv}ReD_2Cl$ int
A′ C−H str.	3090.1	3098.5	3245.6	27	2324.7	2415.4	20
A′ ReH_2 str.	2047.7	2079.6	2144.5	72	1479.8	1521.9	38
A′ C≡Re str.		1063.4	1078.3	8		1027.4	7
A′ HCRe bend		785.5	833.2	3		644.8	3
A′ ReH_2 wag	593.5, 591.2	586.1	618.8	73		449.6	21
A′ ReH_2 scis.		381.1	422.1	2		356.9	65
A′ ReCl str.		347.2	350.8	63		290.4	8
A′ CReCl bend		134.4	140.4	3		130.8	3
A″ ReH_2 str.	2026.1	2053.3	2113.4	35	1459.0	1499.4	19
A″ HCRe bend		837.4	852.6	5		668.3	4
A″ ReH_2 twist	616.6	607.4	636.6	45	437.4?	452.4	22
A″ ReH_2 rock		127.7	220.9	5		162.9	3

[a] Observed in an argon matrix. Frequencies and intensities (km/mol) are from harmonic DFT calculations except where otherwise noted. $HC{\equiv}ReH_2Cl$ has a C_s structure with two equal Re−H bonds. The symmetry notations are based on the C_s structure. [b] Calculated anharmonic frequencies.

with the Re + CH_4 case. The most likely CH_3−ReF (sextet state), CH_2=ReHF (quartet state), and $HC{\equiv}ReH_2F$ (doublet state) products in their ground states are 47, 50, and 63 kcal/mol lower in energy than the reactants, respectively. Furthermore, CH−ReCl (S), CH_2=ReHCl (Q), and $HC{\equiv}ReH_2Cl$ (D) are 51, 52, and 64 kcal/mol more stable than the reactants, respectively, and CH_3−ReBr (S) and CH_2=ReHBr (Q), and $HC{\equiv}ReH_2Br$ (D) are 52, 53, and 64 kcal/mol lower than the reactants, respectively. Regardless of halogen size, the methylidyne complex is the most stable among the most plausible products. Furthermore, the observed and calculated methylidyne frequencies are in good agreement, as shown in Tables 2, 3, and 4. The anharmonic correction improves the agreement with the observed frequencies for C−H and Re−H stretching modes, but not for low frequency bending modes with more complicated potential functions.

Shown in Figure 2 are the methyl halide spectra in the low frequency region. The strongest Re−F stretching absorptions, split by the matrix at 573.2 and 566.4 cm^{-1}, show very small ^{13}C shifts of −0.6 cm^{-1}. The Re−F stretching mode is, in fact, highly mixed with the ReH_2 wagging and HCRe bending modes, and DFT calculations predict that deuterium substitution leads to a blue shift (34.3 cm^{-1}), as shown in Table 2 because of changes in mode mixing in this region upon deuterium substitution. The CD_3F spectra (Figure 2 (i−k)) show the strong Re−F stretching absorption at 608.5 cm^{-1}. Observation of this unusual blue shift upon deuteration further substantiates the formation of $HC{\equiv}ReH_2F$ because similar blue shifts are not expected upon deuteration of CH_3−ReF and CH_2=ReHF.

Table 4. Observed and Calculated Fundamental Frequencies (cm^{-1}) of $HC{\equiv}ReH_2Br$ Isotopomers in the Ground $^2A'$ Electronic State[a]

approximate description	$HC{\equiv}ReH_2Br$ obs	$HC{\equiv}ReH_2Br$ anharm[b]	$HC{\equiv}ReH_2Br$ harm	$HC{\equiv}ReH_2Br$ int	$DC{\equiv}ReD_2Br$ obs	$DC{\equiv}ReD_2Br$ harm	$DC{\equiv}ReD_2Br$ int
A′ C−H str.	3089.8	3095.3	3245.2	27	2324.4	2415.1	21
A′ ReH_2 str.	2043.9	2081.5	2138.6	85	1478.1	1517.6	44
A′ C≡Re str.		1061.9	1077.1	9		1026.2	9
A′ HCRe bend		819.1	825.3	4		640.7	3
A′ ReH_2 wag	592.6	628.1	609.5	85		438.5	37
A′ ReH_2 scis.		585.3	379.2	0		274.6	3
A′ ReBr str.		246.2	242.0	30		235.2	27
A′ CReBr bend		138.3	125.8	3		116.3	3
A″ ReH_2 str.		2060.9	2106.5	35		1494.5	18
A″ HCRe bend		843.7	847.6	6		665.4	5
A″ ReH_2 twist	[c]	659.2	623.6	43		442.5	21
A″ ReH_2 rock		482.5	172.1	5		129.4	2

[a] Observed in an argon matrix. Frequencies and intensities (cm^{-1}) are for harmonic DFT calculations except where otherwise noted. $HC{\equiv}ReH_2Br$ has a C_s structure with two equal Re−H bonds. The symmetry notations are based on the C_s structure. [b] Calculated anharmonic frequencies. [c] Covered by precursor band.

The absorptions at 632.3 and 612.7 cm^{-1} in the CH_3F spectra (Figure 1 (a and b)) have their ^{13}C counterparts at 631.8 and 612.5 cm^{-1}, but the D counterparts are not observed because of their low frequency. They are assigned

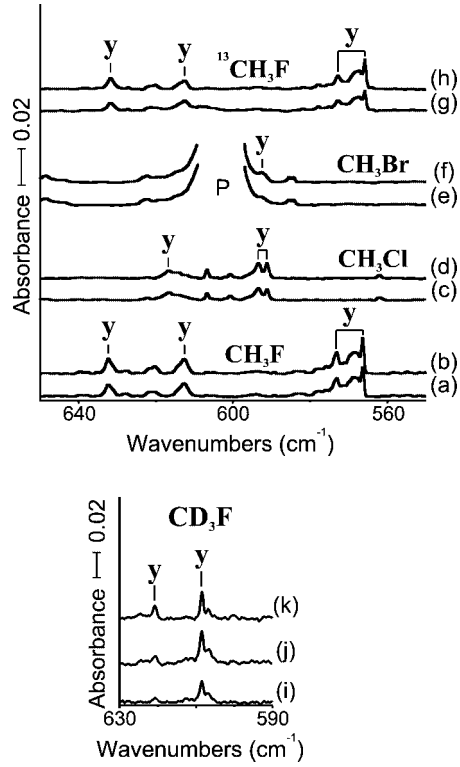

Figure 2. The ReH_2 wagging and twisting and Re−F stretching regions for the laser-ablated Re atom reaction product with CH_3X (X = F, Cl, and Br) and CD_3F in excess argon at 8 K and their variation on UV (240 < λ < 380 nm) photolysis. (a) Re + 0.5% CH_3F in Ar codeposited for 1 h. (b) After photolysis. (c) Re + 0.5% CH_3Cl in Ar codeposited for 1 h. (d) After photolysis. (e) Re + 0.5% CH_3Br in Ar codeposited for 1 h. (f) After photolysis. (g) Re + 0.5% $^{13}CH_3F$ in Ar codeposited for 1 h. (h) After photolysis. (i) Re + 0.5% CD_3F in Ar codeposited for 1 h. (j) After photolysis. (k) After annealing to 28 K. The labels **y** and P stand for the methylidyne product and precursor absorptions, respectively.

to the ReH_2 twisting and wagging modes. The absorption at 620.7 cm^{-1} in the CD_3F spectra is attributed to the HCRe bending mode, whereas the H and ^{13}C counterparts are not observed because of the low intensities, as shown in Table 2. The observed low frequency absorptions all support formation of HC≡ReH_2F.

In the CH_3Cl spectra, the absorptions at 616.6 and 593.5 cm^{-1} are attributed to the ReH_2 twisting and wagging modes of HC≡ReH_2Cl, and a weak absorption at 437.4 cm^{-1} is tentatively assigned to the ReD_2 twisting mode. The Re−Cl and Re−Br stretching bands are too low in frequency to observe. The only absorption, at 592.6 cm^{-1}, in the CH_3Br spectra is assigned to the ReH_2 wagging mode, whereas the ReH_2 twisting absorption is most likely covered by the strong C−Br stretching band of the precursor.

The ReH_2 stretching absorptions of HC≡ReH_2X are more difficult to observe because of their relatively lower intensities than those of previously studied C−H activation products[8] and interfering bands in the region including precursor overtones and metal cluster absorptions. The antisymmetric ReH_2 stretching absorption of HC≡ReH_2F is observed at 2041.0 cm^{-1} in Figure 3 whereas the symmetric stretching absorption is probably covered by the precursor C−F stretching overtone at 2063.4 cm^{-1}. The ^{13}C counterparts are observed at 2063.7 and 2040.4 cm^{-1} and the D counterparts

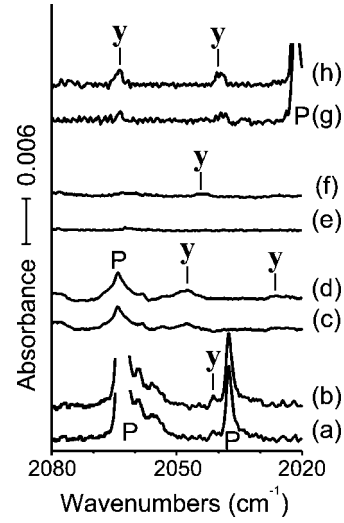

Figure 3. Re−H stretching regions for the laser-ablated Re atom reaction product with CH_3X (X = F, Cl, and Br) in excess argon at 8 K and their variation on UV (240 < λ < 380 nm) photolysis. (a) Re + 0.5% CH_3F in Ar codeposited for 1 h. (b) After photolysis. (c) Re + 0.5% CH_3Cl in Ar codeposited for 1 h. (d) After photolysis. (e) Re + 0.5% CH_3Br in Ar codeposited for 1 h. (f) After photolysis. (g) Re + 0.5% $^{13}CH_3F$ in Ar codeposited for 1 h. (h) After photolysis. The labels **y** and P stand for the methylidyne product and precursor absorptions, respectively.

at 1480.2 and 1459.2 cm^{-1} (not shown) (H/D ratios of 1.394 and 1.398).

The absorptions at 2047.7 and 2026.1 cm^{-1} in the CH_3Cl spectra have their D counterparts at 1479.8 and 1459.0 cm^{-1} (H/D ratios of 1.384 and 1.389) and are assigned to the ReH_2 symmetric and antisymmetric absorptions of HC≡ReH_2Cl. Only a weak absorption is observed at 2043.9 cm^{-1} in the CH_3Br spectra, and it is assigned to the symmetric ReH_2 stretching absorption of HC′ReH_2Br. The D counterpart is found at 1478.1 cm^{-1} (H/D ratio of 1.383).

Re + CH_2X_2. Parallel investigations were done with methylene halides. Figure 4 shows the C−H stretching and low frequency regions of the IR spectra from reactions of Re with CH_2F_2 and CH_2FCl isotopomers, and the observed frequencies are compared with the calculated values in Table 5. The product absorptions remain almost unchanged on visible photolysis but double upon UV photolysis. Clearly, fluorine substitution for hydrogen bonded to Re leads to an increase in the methylidyne C−H stretching frequency, which is ∼100 cm^{-1} higher than the precursor C−H stretching frequency. We find 18.4 and 15.3 cm^{-1} increases in frequency from HC≡ReH_2F and HC≡ReH_2Cl to HC≡$ReHF_2$ and HC≡ReHFCl, respectively. The ^{13}C substitution of CH_2FCl results in a 11.0 cm^{-1} red shift in the C−H stretching frequency of the product (12/13 ratio of 1.0036), but unfortunately, the product C−D stretching absorption in the CD_2FCl spectrum is covered by the CO_2 impurity absorptions.

The Re−F stretching absorptions are observed at 628.2, 629.0, 631.4, and 628.6 cm^{-1} for HC≡$ReHF_2$, HC≡ReHFCl, H^{13}C≡ReHFCl, and DC≡ReDFCl, respectively, and are relatively insensitive to isotopic and halogen substitution. The in- and out-of-plane C−H bending absorptions are also observed on the blue and red sides of the Re−F stretching bands, and the C−D counterparts are observed in the further

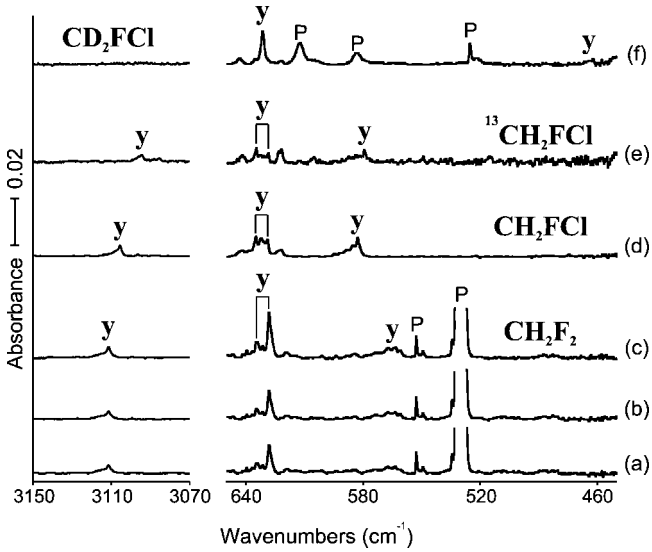

Figure 4. Re−H and low frequency regions for laser-ablated Re atom reaction product with CH_2F_2 and CH_2FCl isotopomers in excess argon at 8 K. (a) Re + 0.5% CH_2F_2 in Ar codeposited for 1 h. (b) After visible (λ > 420 nm) photolysis. (c) After UV (240 < λ < 380 nm) photolysis. (d) After visible and UV photolysis following codeposition Re with 0.5% CH_2FCl in Ar codeposited for 1 h. (e) After visible and UV photolysis following deposition of Re with 0.5% $^{13}CH_2FCl$ in Ar for 1 h. (f) After visible and UV photolysis following deposition of Re with 0.5% CD_2FCl in Ar for 1 h. The labels **y** and P designate the methylidyne product absorption and the absorption in the precursor spectrum, respectively.

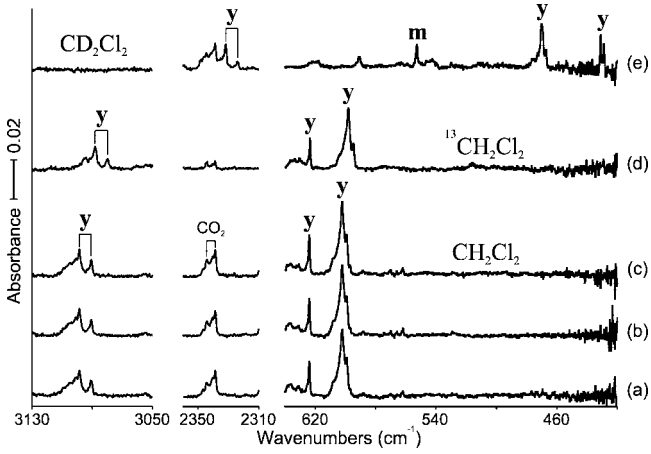

Figure 5. Re−H and D stretching and low frequency regions for laser-ablated Re atom reaction product with CH_2Cl_2 isotopomers in excess argon at 8 K. (a) Re + 0.5% CH_2Cl_2 in Ar codeposited for 1 h. (b) After visible (λ > 420 nm) photolysis. (c) After UV (240 < λ < 380 nm) photolysis. (d) After visible and UV photolysis following codeposition Re with 0.5% $^{13}CH_2Cl_2$ in Ar codeposited for 1 h. (e) After visible and UV photolysis following deposition of Re with 0.5% CD_2Cl_2 in Ar for 1 h. The product absorptions increase only slightly in the process of photolysis. The labels **y** and **m** stand for the methylidyne and methylidene product absorptions, respectively.

low frequency region. The single C−H stretching absorptions on the blue sides of the precursor C−H stretching bands and other product absorptions show a good correlation with the predicted values, which substantiates the formation of $HC{\equiv}ReHX_2$ methylidynes as the primary product.

The IR spectra of CH_2Cl_2 and its isotopomers are shown in Figure 5, and the frequencies are listed in Table 6. The C−H stretching absorptions are split by the matrix at 3098.6 and 3090.7 cm^{-1} with ^{13}C counterparts at 3088.2 and 3079.7 cm^{-1} (12/13 ratios of 1.0034 and 1.0036) and D counterparts at 2331.9 and 2324.0 cm^{-1} (H/D ratios of 1.329 and 1.330). The in- and out-of-plane C−H bending absorptions are observed at 623.9 and 602.2 cm^{-1}, the ^{13}C counterparts are at 623.4 and 598.0 cm^{-1} (12/13 ratios of 1.0008 and 1.0070), and the D counterparts are at 446.0 and 469.8 cm^{-1} (H/D ratios of 1.399 and 1.282). Weak bands were also observed at 2103.0 and 1509.6 cm^{-1} for the Re−H and Re−D stretching modes (H/D ratio 1.393), which is the highest such mode we have found for these compounds. The observed and calculated frequencies and isotopic frequencies are in very good agreement, as shown in Table 6. Finally, the observed C−H stretching and bending absorptions with appropriate isotopic shifts substantiate formation of the methylidyne product, $HC{\equiv}ReHCl_2$ in the reaction of Re with methylene chloride.

Figure 5 also shows a sharp absorption at 552.5 cm^{-1} marked "**m**". Previous studies indicate that a methylidyne product is often formed after its methylidene derivative.[8] In this case, the $CH_2{=}ReCl_2$ methylidene is 9.2 kcal/mol higher in energy than the methylidyne product. It is, therefore, probable that the absorption originates from the CD_2 wagging mode of $CD_2{=}ReCl_2$(Q), the only strong absorption of the product (calculated at 610.0 cm^{-1}) in our observation range. However, unfortunately the CH_2 counterpart, predicted at 775.3 cm^{-1}, is covered by the strong precursor C−Cl stretching absorption.

Re + C_2H_6. Shown in Figure 6 are spectra from the Re and ethane reaction product in the Re−H stretching region. The product absorptions marked **y** remain unchanged on visible (λ > 420 nm) irradiation but increase ∼15% upon UV (240 < λ < 380 nm) irradiation. They increase another 10% upon full arc (λ > 220 nm) irradiation and sharpen in the early stage of annealing. Similar to those in the CH_4 spectra, unique strong absorptions split by the matrix are observed at 1786.3 and 1780.5 cm^{-1}, which are 23.6 and 23.5 cm^{-1} lower than the corresponding frequencies in the CH_4 spectrum, respectively. Their D counterparts are observed at 1285.9 and 1281.6 cm^{-1} (H/D ratios of 1.389), which are 16.7 and 16.5 cm^{-1} lower, respectively, than the corresponding frequencies in the CD_4 spectrum. Substitution with deuterium appropriately lowers the hydrogen stretching frequencies.

The methylidyne complex ($CH_3C{\equiv}ReH_3$) is again the most stable among the plausible products of Re + C_2H_6. The monohydrido insertion product ($CH_3CH_2{-}ReH$) in its quartet ground-state is 0.1 kcal/mol higher in energy than the reactants, and its Re−H stretching frequency is predicted at 2072.4 cm^{-1}, which is almost 300 cm^{-1} higher than the observed values. The methylidene $CH_3{-}CH{=}ReH_2$ (Q), another plausible product, is 3.2 kcal/mol lower than the reactants, and the Re−H stretching bands are predicted at 1927.1 and 1848.9 cm^{-1} with an intesity ratio of about 1:2. Cyclic $(CH_2)_2ReH_2$ (Q) is 12 kcal/mol more stable than the reactants, and the Re−H stretching frequencies are predicted at 2013.2 and 1956.6 cm^{-1} with about 40% more intensity for the former. On the other hand, the methylidyne complex ($CH_3C{\equiv}ReH_3$) is 18 kcal/mol more stable than the reactants, and the frequency of the strongest Re−H stretching band is

Table 5. Observed and Calculated Fundamental Frequencies (cm^{-1}) of $HC{\equiv}ReHF_2$ and $HC{\equiv}ReHFCl$ Isotopomers in the Doublet Ground States[a]

	$HC{\equiv}ReHF_2$			$HC{\equiv}ReHFCl$			$DC{\equiv}ReDFCl$			$H^{13}C{\equiv}ReHFCl$		
approximate description	obs	harm	int	obs	harm	int	obs	harm	int	obs	harm	int
C−H str.	3111.3	3269.0	41	3105.4	3264.6	41		2430.2	29	3094.4	3252.4	40
Re−H str.		2206.8	16		2205.2	13		1564.5	7		2205.2	13
C≡Re str.		1091.5	11		1089.5	9		1038.0	7		1053.4	8
CReH bend		900.2	3		888.9	3		698.2	3		881.3	3
ReCH ip bend	634.4	664.7	57	634.9	662.8	57	462.0	481.2	37	634.6	662.1	57
Re−F str.	628.2	628.5	135	629.0	627.9	100	631.4	627.6	132	628.6	627.8	103
ReCH oop bend	564.8	588.0	129	582.8	609.9	119	450.7	461.5	40	579.4	606.2	115
Re−Cl(F) str.		631.3	72		381.4	47		381.1	46		381.3	48
HReFCl deform		253.7	6		335.5	7		242.3	4		335.3	7
CReHF deform		225.9	0		218.4	2		203.4	2		213.4	2
CReFCl deform		184.9	3		151.2	1		145.3	1		149.7	1
ReFCl bend		147.7	5		121.3	2		119.8	2		121.1	2

[a] Observed in an argon matrix. Frequencies and intensities (km/mol) are for harmonic DFT calculations except where otherwise noted. $HC{\equiv}ReHF_2$ has a C_s structure with two equal Re−F bonds. The symmetry notations are based on the C_s structure.

Table 6. Observed and Calculated Fundamental Frequencies (cm^{-1}) of $HC{\equiv}ReHCl_2$ Isotopomers in the Ground $^2A''$ Electronic State[a]

	$HC{\equiv}ReHCl_2$			$DC{\equiv}ReDCl_2$			$H^{13}C{\equiv}ReHCl_2$		
approximate description	obs	harm	int	obs	harm	int	obs	harm	int
A′ C−H str.	3098.6, 3090.7	3261.1	41	2331.9, 2324.0	2427.4	25	3088.2, 3079.7	3248.9	
A′ ReH str.	2103.0	2200.6	10	1509.6	1561.2	5	2103.0	2200.6	
A′ C≡Re str.		1086.0	6		1034.6	5		1049.9	
A′ HCRe bend		882.6	3		692.8	3		875.1	
A′ HReC bend	623.9	657.0	46	446.0	490.1	52	623.4	656.6	
A″ HCRe bend	602.2, 599.1	632.5	90	469.8, 467.2	468.4	22	598.0, 594.8	628.1	
A″ $ReCl_2$ str.		385.3	101		385.0	99		385.2	
A′ $ReCl_2$str		370.8	13		370.4	14		173.1	
A″ ReH wag		353.1	6		254.0	4		2126.3	
A″ CReCl bend		201.8	3		184.8	2		845.4	
A′ $ReCl_2$ bend		128.8	0		124.0	0.3		639.1	
A′ $ReCl_2$ def		97.6	0		96.3	0.3		255.1	

[a] Observed in an argon matrix. Frequencies and intensities (km/mol) are for harmonic DFT calculations except where otherwise noted. $HC{\equiv}ReHCl_2$ has a C_s structure with two equal Re−Cl bonds. The symmetry notations are based on the C_s structure.

Table 7. Methylidyne C−H Stretching Frequencies and Bond Properties[a]

properties	$HC{\equiv}CH$	$HC{\equiv}ReH_3$	$HC{\equiv}ReH_2F$	$HC{\equiv}ReH_2Cl$	$HC{\equiv}ReH_2Br$	$HC{\equiv}ReHF_2$	$HC{\equiv}ReHFCl$	$HC{\equiv}ReHCl_2$	CH_3CH_3
obs.	3284[b]	3101.8	3092.9	3090.1	3089.8	3111.3	3105.4	3098.6	2979.3
calc.	3412.3	3264.8	3249.7	3246.1	2145.2	3269.0	3264.6	3261.1	3027.3
obs./calc.	0.962	0.950	0.952	0.952	0.952	0.952	0.951	0.950	0.984
s-character (C-H)[c]	47.82	46.55	45.86	45.65	45.52	47.99	47.18	46.73	23.46
s-character (C-M)[c]	52.34	53.20	53.92	54.18	54.30	51.82	52.62	53.08	29.75
q(H)[d]	0.222	0.179	0.180	0.181	0.181	0.191	0.189	0.190	0.190
q(C)[d]	−0.222	−0.236	−0.283	−0.218	−0.212	−0.294	−0.225	−0.175	−0.570
q(Re)[d]		0.577	0.885	0.608	0.556	1.276	0.962	0.648	
r(C−H) (Å)	1.0617	1.0795	1.0806	1.0810	1.0811	1.0788	1.0792	1.0796	1.0908
R(C−M) (Å)	1.196	1.714	1.742	1.723	1.722	1.719	1.718	1.718	1.527
∠HCRe (°)	180.0	179.1	172.1	172.8	173.3	179.2	179.2	179.9	111.3

[a] Frequencies are in cm^{-1}. Harmonic frequencies computed with B3LYP, 6–311++G(3df, 3pd), and the SDD core potential. [b] Reference 22. [c] s-Character of the carbon atom in the bond. [d] Natural charge.

predicted at 1829.9 cm^{-1} as shown in Table 8, which is 2.4% higher than the observed value and is appropriate for the B3LYP calculation.[21]

Two more Re−H stretching bands are observed at 1953.5 and 1900.1 cm^{-1}, as shown in Figure 6, and their D counterparts are observed at 1406.0 and 1359.8 cm^{-1} (H/D ratios of 1.389 and 1.397, respectively). The observed three hydrogen stretching absorptions, one with much lower frequency, support a principal product containing a ReH_3 group with unequal Re−H bonds, parallel to the case of Re + CH_4. The observed Re−H stretching frequencies reasonably match with the predicted frequencies for $CH_3C{\equiv}ReH_3$. Extensive calculations are also carried out for other plausible products, such as $(CH_3)_2Re$, CH_2CHReH_3, $CHCHReH_4$, and $HC{\equiv}CReH_5$, but none of them is predicted to be as stable as $CH_3C{\equiv}ReH_3$, and none reproduces the observed results in the Re−H stretching region.

Another absorption at 701.4 cm^{-1} (not shown) has its D counterpart at 517.0 cm^{-1} (H/D ratio of 1.357) and is assigned to the ReH_3 deformation mode. A weak absorption observed at 449.7 cm^{-1} is tentatively assigned to the ReH_3 rocking mode without observation of the D counterpart, which is beyond our observation limit. The observed absorptions, whose frequencies match with those of the bands predicted to be strong for $CH_3C{\equiv}ReH_3$, substantiate formation of the methylidyne complex, parallel to formation of $HC{\equiv}ReH_3$ and its halide derivatives. No other product

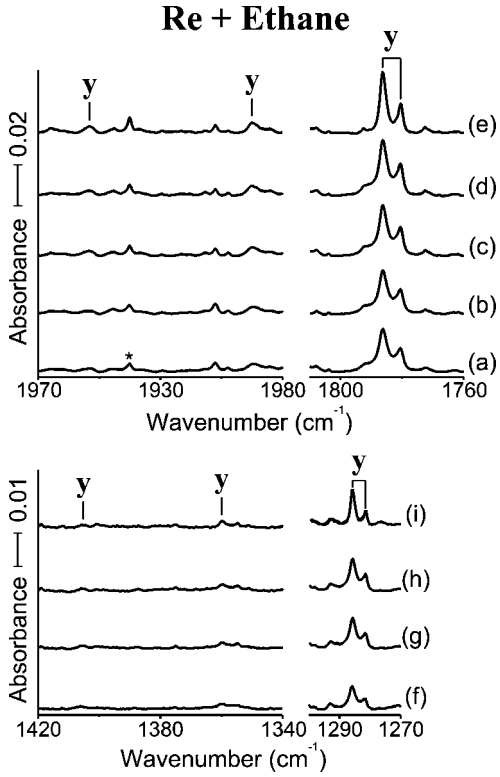

Figure 6. The Re−H and Re−D stretching regions for the laser-ablated Re atom reaction product with ethane in excess argon at 8 K and their variations. (a) Re + 0.5% C_2H_6 in Ar codeposited for 1 h. (b) After photolysis ($\lambda > 420$ nm). (c) After photolysis ($240 < \lambda < 380$ nm). (d) After photolysis ($\lambda > 220$ nm). (e) Annealing to 28 K. (f) Re + 0.5% C_2D_6 in Ar codeposited for 1 h. (g) After photolysis ($240 < \lambda < 380$ nm). (h) After photolysis ($\lambda > 220$ nm). (i) Annealing to 28 K. The **y** and * labels denote the methylidyne product and Re metal cluster absorptions.

species were observed in the Re + C_2H_6 spectra, as in the methane and methyl halide cases.

Methylidyne C−H Stretching Absorptions. The carbon-hydrogen stretching region is normally congested, prohibiting observation of important weak absorptions in this diagnostic region. The simple precursor spectrum and the methylidyne product with no interfering ligand chromophores allow for observation of the elusive C−H stretching band of the H−C≡M moiety. Although in principle, the C−H stretching mode interacts with the C≡M stretching mode, these modes are separated by some 2000 cm^{-1}, and this interaction is minimal. In addition, it is well-known that the hydrogen stretching frequency generally increases with the amount of s character in the C−H bond, and a C−H stretching frequency above 3000 cm^{-1} is normally regarded as evidence for the presence of an adjacent multiple bond.[20] However, the high observed C−H stretching frequency of 3101.8 cm^{-1} is substantially lower than those of acetylene (the antisymmetric stretching band at 3284 cm^{-1} in an argon matrix and the IR-inactive symmetric stretching mode is some 90 cm^{-1} higher).[22] The methylidyne C−H stretching frequencies and related bond properties are summarized in Table 7. The observed C−H stretching frequency decreases in the order of HC≡ReH_3, HC≡ReH_2F, HC≡ReH_2Cl, and HC≡ReH_2Br, and this trend is consistent with the computed s character and bond length values.

Whereas most molecular properties change with the halogen electronegativity, it is interesting that only the variation of the s character in the C−H bond estimated by NBO analysis[10,23] is in line with the trend of the C−H stretching frequencies and the calculated bond lengths as shown in Table 7. The NBO computed s characters of the carbon contribution to the C−H bonds are 47.82, 46.55, 45.86, 45.65, 45.52, and 23.46% for HC≡CH, HC≡ReH_3, HC≡ReH_2F, HC≡ReH_2Cl, HC≡ReH_2Br, and C_2H_6, respectively, and they are compared with the C−H stretching frequencies observed at 3284, 3101.8, 3092.9, 3090.1, 3089.8, and 2979.3 cm^{-1}. Unlike in acetylene, the difference in electronegativity (2.5, 2.1, and 1.9 for C, H, and Re using the Pauling scale, respectively) leads to polarization of the C≡Re bond, which in turn allocates more s character to the polarized C≡Re bond. As a result, the methylidyne C−H bond gains p character and weakens accordingly, as compared to acetylene itself. Although the observed C−H stretching frequency decrease is only 4.1 cm^{-1} in the HC≡ReH_2X series, it is matched by a 0.0005 Å increase in the C−H bond length (Table 7).

This trend continues with the HC≡$ReHF_2$, HC≡ReHFCl, and HC≡$ReHCl_2$ methylidynes, which have higher C−H stretching frequencies and s characters as given in Table 7. The frequency decreases from 3111.3 to 3098.6 cm^{-1} and the s character from 47.99 to 46.73 in this dihalogen series. A similar trend was found within the trihalogen series, but a smaller 3103.8 to 3097.3 cm^{-1} C−H frequency decrease was accompanied by a larger 49.22 to 47.80 s character decrease.[9] In contrast, the highest s character HC≡ReF_3 methylidyne had a 7.5 cm^{-1} lower C−H frequency than HC≡$ReHF_2$, and this reversal is probably due to the greater inductive effect of three fluorine atoms.

Reaction Mechanism. The methylidyne complexes are produced through initial C−H or C−X insertion reactions of Re with methane, methyl halides, methylene halides, and ethane. A Re atom, electronically excited in the laser ablation process or by UV irradiation into the strong 326 nm argon matrix absorption involving the resonance 6s→6p transition,[24,25] executes C−H or C−X insertion, and α-hydrogen migration follows, as given in reaction 1. The increase in product absorptions on UV irradiation along with a decrease in methane overtone absorption further supports the initial step in reaction 1 for Re atoms and methane molecules in close proximity in the argon matrix. Furthermore, the methylidyne complexes are clearly the most stable among the plausible products in all of the Re systems investigated in this study. Nevertheless, the high preference of the C≡Re triple bond is perhaps surprising in consideration of the relatively small energy lowering relative to the next most stable methylidene products, namely 7, 17, 13, 11, and 18

(22) Herzberg, G. *Infrared and Raman Spectra*; D. Van Nostrand: Princeton, New Jersey, 1945.
(23) Reed, A. E.; Curtiss, L. A.; Weinhold, F. *Chem. Rev.* **1988**, *88*, 899.
(24) Klotzbucher, W. E.; Ozin, G. A. *Inorg. Chem.* **1980**, *19*, 376.
(25) Carstens, D. H. W.; Brashear, H.; Eslinger, D. R.; Gruen, D. M. *Appl. Spectrosc.* **1972**, *26*, 184.

Table 8. Observed and Calculated Fundamental Frequencies (cm^{-1}) of $CH_3C{\equiv}ReH_3$ Isotopomers in the Ground $^2A'$ Electronic State[a]

	$CH_3C{\equiv}ReH_3$				$CD_3C{\equiv}ReD_3$		
approximate description	obs	anharm[b]	harm	int	obs	harm	int
A′ ReH_2 str.	1953.5	1985.5	2073.3	101	1406.0	1470.9	55
A′ ReH str.	1786.3, 1780.5	1758.4	1829.9	282	1285.9, 1281.6	1299.9	138
A′ ReH_3 rock	449.7	451.4	477.3	26		338.7	1
A″ ReH_2 str.	1900.1	1936.6	2021.5	55	1359.8	1435.8	29
A″ CH_3 scis.	1425.6	1418.2	1460.5	13	1030.6	1051.4	6
A″ ReH_3 deform	701.4	706.1	763.8	31	517.0	549.2	12

[a] Observed in an argon matrix. Frequencies and intensities (km/mol) are from harmonic DFT calculations except where otherwise noted. $CH_3C{\equiv}ReH_3$ has a C_s structure with two equal Re−H bonds. The symmetry notations are based on the C_s structure. [b] Calculated anharmonic frequencies.

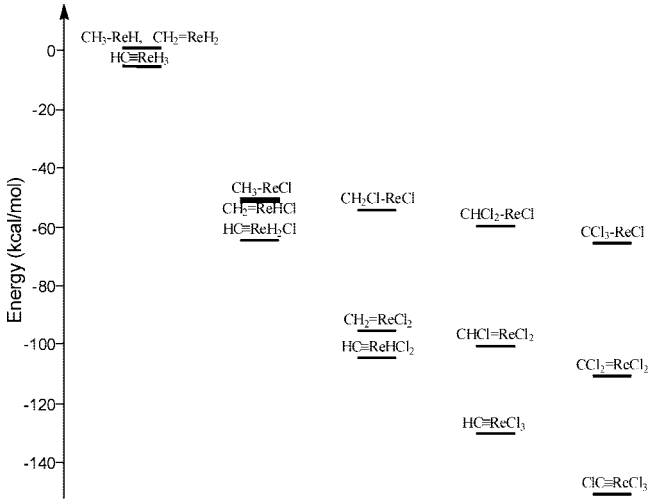

Figure 7. Energies of the insertion, methylidene, and methylidyne complexes relative to the Re atom and halomethane reactants. Notice that the methylidyne product becomes more stable than other complexes as the number of chlorine atoms increases. For the methane reaction the products are quartet, doublet, and doublet states, respectively, and for the halogen derivatives, the products are sextet, quartet, and doublet states, respectively.

kcal/mol in the CH_4, CH_3F, CH_3Cl, CH_3Br, and C_2H_6reactions.

Reaction products some 20 kcal/mol higher than the most stable have often been formed during reactions of transition metal atoms with CH_4 and methyl halides or photolysis afterward and trapped in the solid argon matrix.[8] However, in these Re complexes the dynamics are different, and α-hydrogen migration appears to be faster than relaxation of the energized intermediates in the matrix cage, regardless of the reactant. Also, reaction 1 goes to the lowest energy final methylidyne product. However, for the dihalogen substituted precursors, the methylidene complex is only 9.2 kcal/mol higher in energy than the methylidyne final product, and a small amount of the methylidene intermediate is trapped in the matrix.

$$Re^* + CH_3X \rightarrow [CH_3{-}ReX]^* \rightarrow [CH_2{=}ReHX]^* \rightarrow HC{\equiv}ReH_2X \quad (1)$$

$$Re^* + CH_2X_2 \rightarrow [CH_2X{-}ReX]^* \rightarrow [CH_2{=}ReX_2]^* \rightarrow HC{\equiv}ReHX_2 \quad (2)$$

Figure 8 summarizes the energies of the three steps in these reaction mechanisms as a function of the number of chlorine substituents. The thermodynamic driving force for α-halogen transfer is obvious, and the preference for the methylidyne product is enhanced in the haloform and tetrahalide systems.[9]

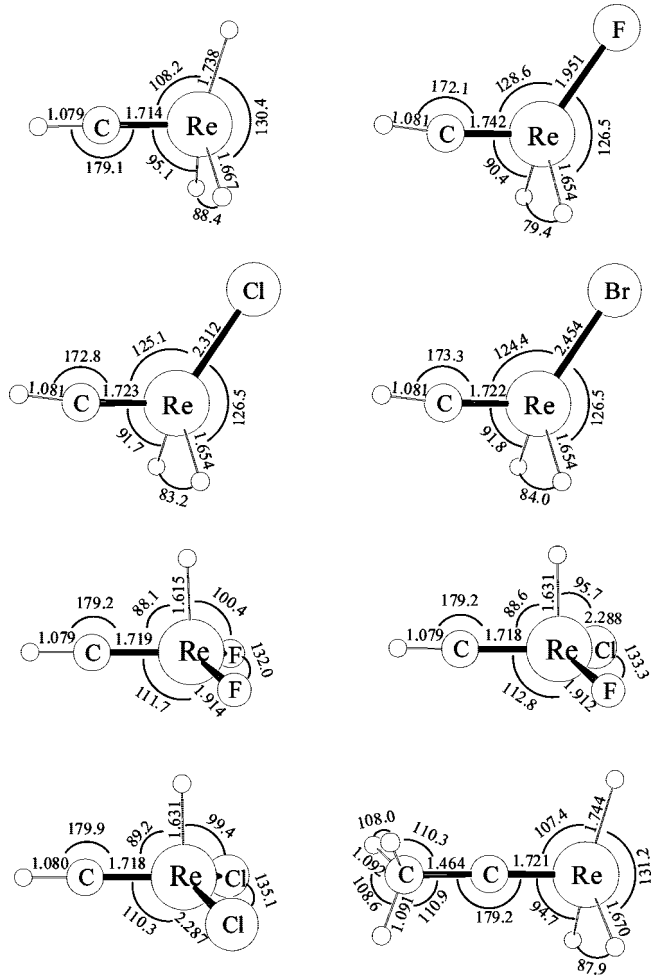

Figure 8. The structures of $HC{\equiv}ReH_3$, $HC{\equiv}ReH_2F$, $HC{\equiv}ReH_2Cl$, $HC{\equiv}ReH_2Br$, $HC{\equiv}ReHF_2$, $HC{\equiv}ReHFCl$, and $HC{\equiv}ReHCl_2$ optimized at the level of B3LYP/6–311++G(3df,3pd)/SDD. The bond lengths and angles are in Å and °. These methylidynes have C_s structures in their $^2A'$ or $^2A''$ ground states (except for $HC{\equiv}ReHFCl$). The $HC{\equiv}ReH_3$ and $CH_3C{\equiv}ReH_3$ complexes have the two equal shorter Re−H bonds and one longer Re−H bond.

Structures. The methylidyne complexes in their doublet ground states, except for the mixed halogen species, all have C_s structures as illustrated in Figure 7. One of the hydrogen atoms bonded to the Re atom in the structures of $HC{\equiv}ReH_3$ and $CH_3C{\equiv}ReH_3$ is tilted more with a longer Re−H bond (lower stretching frequency, higher electron density, and higher absorption intensity) than the other two. It is important to note that the singly occupied HOMO is antibonding in this longer Re−H bond and is bonding in the shorter Re−H bonds. In addition, calculations for $HC{\equiv}ReH_3$ and

$CH_3C{\equiv}ReH_3$ with BPW91/6–311++G(3df,3pd)/SDD, MP2/6–311++G(2d,p)/SDD, and the more rigorous CCSD/6–311++G(3df,3pd)/SDD for Re and (CCSD/6–311++G(2d,p)/SDD for $CH_3C{\equiv}ReH_3$) also give similar C_s structures with a longer Re−H bond (1.735, 1.702, and 1.719 Å, respectively, for $HC{\equiv}ReH_3$ and 1.741, 1.740, and 1.742 Å, respectively, for $CH_3C{\equiv}ReH_3$). These rhenium methylidyne complexes are particularly interesting because of the unique C≡Re triple bonding and the distorted structures about the metal center, which is due to the Jahn–Teller effect,[26] as has been described in detail for the $XC{\equiv}ReX_3$ and $HC{\equiv}ReX_3$ complexes.[9]

The nondegenerate $^2A'$ ground states and asymmetric molecular structures of $HC{\equiv}ReH_3$ and $CH_3C{\equiv}ReH_3$ at the Re centers are due to the lifting of 3-fold symmetry by Jahn–Teller distortion driven by an open shell e-symmetry orbital,[26] which is not present in the symmetrical singlet state $HC{\equiv}WH_3$ complex.[27] We have shown that the spin–orbit coupling effects are significant for the $XC{\equiv}ReX_3$ and $HC{\equiv}ReX_3$ complexes but are not large enough to quench the large Jahn–Teller distortion.[9]

In the monohalogen derivatives, the halogen atoms replace the hydrogen atom with the longer Re−H bond, and the equivalent Re−H bonds are even shorter (1.654 Å) as shown in Figure 8. The singly occupied HOMO is antibonding for this longer bond, as shown in the TOC graphic. In the present series of methylidyne molecules, the shortest Re−H bond is found for $HC{\equiv}ReHF_2$, with the highest Re−H stretching frequency (2103.0 cm^{-1}) where the inductive effect of fluorine on the Re orbitals is again apparent. The C≡Re bond and the Re−F bonds become progressively shorter as the number of fluorine ligands at the Re center is increased from 1 to 3.[9]

The methylidyne H−C bond lengths of 1.079–1.081 Å are compared to those of 1.076 and 1.081 Å for H−C≡W[4] and $HC{\equiv}WH_3$,[27] respectively, and the C-H stretching frequency for the latter is calculated to be 29 cm^{-1} lower with half of the infrared intensity than that of $HC{\equiv}ReH_3$. The C≡Re bond length increases substantially upon substitution of F (from 1.714 to 1.742 Å) due to the reduced electron density in the bond or alternatively increased positive charge and contraction of 5d valence orbitals, and the C≡Re bond then decreases with increasing halogen size, indicating that the C≡Re bond becomes stronger with a lower ligand electronegativity. The calculated C≡Re bond lengths of 1.714–1.742 Å are compared with the C≡M bond lengths of 1.755, 1.737, and 1.77(1) Å measured for the (η^5-C_5Me_5)$(Br)_3Re{\equiv}CC(CH_3)_3$,[28] H−C≡W,[4] and BrW≡CH(dmpe-d_{12})$_2$ compounds,[7] respectively.

Conclusions

The $^2A'$ ground-state rhenium methylidyne complexes, $HC{\equiv}ReH_3$, $HC{\equiv}ReH_2F$, $HC{\equiv}ReH_2Cl$, $HC{\equiv}ReH_2Br$, and $CH_3C{\equiv}ReH_3$ are exclusively produced in reactions of laser-ablated Re atoms with the corresponding alkane and methyl halide precursors. Analogous $^2A''$ methylidynes $HC{\equiv}ReHF_2$, $HC{\equiv}ReHFCl$, and $HC{\equiv}ReHCl_2$ are observed in the reaction with methylene halides. The relative stabilities of the methylidyne complexes among the plausible reaction products are reproduced by DFT calculations. The observed vibrational characteristics are in very good agreement with the calculated values for the methylidyne complexes within the limits of the harmonic approximation. Particularly, the uniquely strong Re−H absorptions with relatively low frequencies observed in CH_4 and C_2H_6 spectra are mostly due to stretching of the hydrogen atom with the longer Re−H bond length where Jahn–Teller distortion[26] is responsible for reduction of 3-fold symmetry in the $HC{\equiv}ReH_3$ and $CH_3C{\equiv}ReH_3$ complexes.

The methylidyne C−H stretching absorptions, which are seldom observed because of low intensity and interference from other hydrogen stretching absorptions, are clearly observed with isotopic shifts in the matrix-isolated product spectra. The C−H stretching frequency is ∼100 cm^{-1} higher than those of normal saturated hydrocarbons but is substantially lower than that of acetylene. The observed frequency decreases in the order of $HC{\equiv}ReH_3$, $HC{\equiv}ReH_2F$, $HC{\equiv}ReH_2Cl$, and $HC{\equiv}ReH_2Br$, which matches with the calculated frequencies and bond lengths for these species. Natural bond orbital (NBO) analyses reveal that the methylidyne C−H stretching frequency increases steadily with the amount of s character in the C−H bond. Polarization in the C≡Re bond apparently increases the s character in the triple bond, which in turn decreases the s character in the C−H bond instead and lowers the methylidyne C−H stretching frequency. The C−W bond is polarized even more with calculated natural charges of −0.34 and +0.75, and the s character for the H−C bond is reduced to 45.6%, which results in the longer and lower frequency C−H bond in the $HC{\equiv}WH_3$ molecule.[27]

Trihydrido complexes of Re have been proposed as intermediates in the synthesis of dihydrido complexes.[10b] We have prepared the simple, trihydrido ($HC{\equiv}ReH_3$ and $CH_3C{\equiv}ReH_3$) as well as dihydrido halide ($HC{\equiv}ReH_2X$) and monohydrido dihalide ($HC{\equiv}ReHX_2$) methylidyne complexes in reactions of Re with the simple halomethanes and ethane and have trapped them in solid argon for spectroscopic analysis.

Acknowledgment. We gratefully acknowledge financial support from NSF Grant CHE 03-52487 to L. A.

IC701505W

(26) Herzberg, G., *Electronic Spectra of Polyatomic Molecules*; D. Van Nostrand: Princeton, New Jersey, 1966.
(27) Cho, H.-G.; Andrews, L.; Marsden, C. *Inorg. Chem.* **2005**, *44*, 7634 and references therein (W + CH_4).
(28) (a) Felixberger, J. K.; Kiprof, P.; Herdtweck, E.; Herrmann, W. A.; Jakobi, R.; Gutlich, P *Angew. Chem., Int. Ed. Engl.* **1989**, *28*, 334. (b) Herrmann, W. A.; Felixberger, J. K.; Anwander, R.; Herdtweck, E.; Kiprof, P.; Riede, J. *Organometallics* **1990**, *9*, 1434.